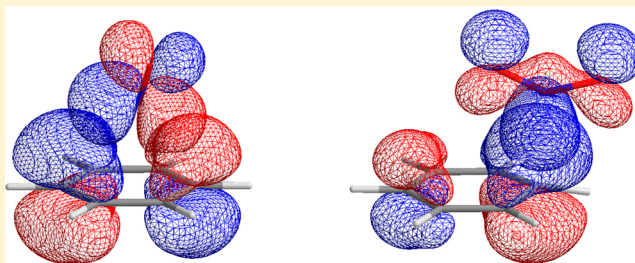


Electron Transfer in Electrophilic Aromatic Nitration and Nitrosation: Computational Evidence for the Marcus Inverted Region

Zhenhua Chen and Yirong Mo*

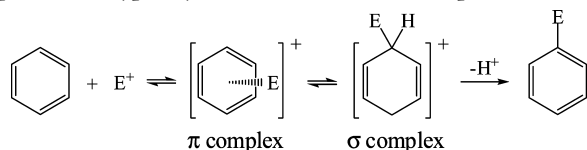
Department of Chemistry, Western Michigan University, Kalamazoo, Michigan 49008, United States

ABSTRACT: Electrophilic aromatic nitrosation and nitration are among the most important electron transfer (ET) reactions. According to the electron transfer theory, an ET process can be described with two electron-localized diabatic states, and the electronic coupling between these two states, together with the organization energy and reaction energy, determine the ET efficiency. A proper definition of the strictly electron-localized states thus is the key. Here we used the valence bond theory to derive the diabatic states and probe the interactions of NO^+ and NO_2^+ with benzene and identify the origin of their significant difference in reactivity. Results show that the high deformation cost for NO_2^+ overshadows the fact that it has much high charge transfer interaction in $[\text{C}_6\text{H}_6, \text{NO}_2]^+$. While NO^+ uses π orbitals to bind benzene and the orbital switch results in a high barrier from π - to σ -complex, NO_2^+ uses a vacant $\sigma(\text{Nsp}^2)$ orbital, making the transition nearly barrierless. Significantly, we found that the post-ET state $[\text{C}_6\text{H}_6^+ - \text{NO}]$ is more stable than the prior-ET state $[\text{C}_6\text{H}_6, \text{NO}^+]$. Energy profiles with respect to the distance between the electrophile and the benzene confirm that the ET reaction of benzene and NO^+ falls in the Marcus inverted region, and the outer-sphere ET occurs at ~ 2.6 Å with the electronic coupling energy of 1.06 eV, compared with the experimental estimate 1.4 ± 0.5 eV.



INTRODUCTION

Electrophilic aromatic substitution (EAS) refers to the classic organic processes where a proton is replaced by an electrophile.¹ As a synthetically and industrially important reaction type, EAS is typically elucidated with three steps as follows



In this general reaction mechanism, the complexation of the electrophile E^+ with the aromatic ring, resulting in an encounter π complex, is usually rapid and reversible. To make the substitution occur, the electrophile needs to further approach the aromatic ring and be bonded to the carbon at the site of substitution, leading to a cationic intermediate called σ (or Wheland) complex. This σ intermediate, which has been experimentally observed,^{2,3} is usually unstable and highly reactive and thus governs the reactivity and regioselectivity of EAS reactions. A mechanism of single-electron transfer (SET) from the aromatics to electrophile has been proposed and recognized.^{4,5}

One ubiquitous kind of important reactions in the family of EAS is the electrophilic aromatic nitrosation and nitration which have been extensively studied both experimentally^{6–12} and computationally,^{13–17} notably by the Eberson group^{18–20} and the Kochi group.^{21–24} Nitrations are kinetically controlled with the generation of σ complexes as the rate-limiting step, and the nitronium ion (NO_2^+) is largely considered to be the

active electrophile.²⁵ Similarly, the nitrosonium ion (NO^+) is the active reactant in the nitrosylation of arenes.¹⁰ Intriguingly, although both electrophiles have similar inherent physical properties such as the reversible potentials and ionization energies,²⁶ their chemical reactivities toward various aromatic donors are dramatically different, and NO_2^+ is estimated to be 10^{14} times more effective than NO^+ in EAS reactions.²⁷ Gwaltney et al. have carefully investigated this disparity via molecular orbital (MO) and Marcus–Hush theories.²⁶ They mapped out the bimolecular interactions of benzene with NO_2^+ and NO^+ along the reaction coordinates at the CCSD(T)/6-31G** theoretical level and identified that there are two reactive intermediates in nitration (π and σ complexes) but only one in nitrosation (π complex with the σ complex as a transition state at much high energy level).

The key to the understanding of the different reactivity of NO_2^+ and NO^+ toward arene thus lies in the elucidation of the bonding nature of their stable π complexes, which are the minimum states in energy profiles and also called electron transfer complexes²⁴ and the prototypes for the electron transfer theory.²⁸ Experimentally, the existence of electron transfer complexes has been well established by X-ray crystallography coupled to the IR spectroscopic analysis and confirmed by NMR analyses.²¹ Following the two-state model developed by Mulliken, Marcus, Hush, and many others,^{29–31} the electron transfer complex $[\text{ArH}, \text{E}]^+$ of an aromatic ring

Received: July 15, 2013

Published: August 19, 2013



$$H_{\text{DA}} = \mathbf{H}_{\text{aa/bb}} - E_1 \quad (7)$$

Structural contributions of the diabatic states to the adiabatic ground state can be evaluated with the Coulson–Chirgwin formula which is an equivalent of the Mulliken population analysis.

It should be noted that for the $[\text{C}_6\text{H}_6\text{NO}]^+$ π complex, the N–O axis is almost vertical to the plane of benzene and above the center of the aromatic ring. As both the highest occupied MO (HOMO) of benzene and the lowest unoccupied MO (LUMO) of NO^+ are degenerate and of π symmetry, and the electron transfer occurs from π (benzene) to π^* (NO^+), there are two possible routes (if we approximate the vertical direction as z -axis, the two routes are along x - and y -axis, respectively). Accordingly, there are two nearly degenerate covalent structures (eq 5), where the block-localized orbitals $\{\phi\}$ are dominated by either p_x or p_y orbitals on NO^+ with e_{1g} degenerate orbitals on benzene. A complete description of the post-ET state $[\text{C}_6\text{H}_6^+-\text{NO}]$ should include two VB functions, as we did in this work. For the $[\text{C}_6\text{H}_6\text{NO}_2]^+$ π -complex, however, NO_2^+ bends and uses one σ orbital to interact with benzene, thus one covalent structure is sufficient to describe the electron transfer process.

The geometries of complexes and monomers were optimized at the B3LYP/cc-pVTZ level with an in-house version of the quantum mechanical software GAMESS⁶³ with the function of BLW computations. Vibrational frequencies are computed with a scaling factor of 0.9682.⁶⁴ Computations in the framework of the two-state theory were performed with the Xiamen Valence Bond (XMVB) program,⁶⁵ with the B3LYP/cc-pVTZ geometries and the 6-31G(d,p) basis set.

RESULTS

Formation of π Complexes. The geometries of benzene complexed with NO^+ and NO_2^+ have been extensively documented in the literature. However, one unique feature of the BLW method is the geometry optimization of structures where electron transfer is hypothetically deactivated.⁶⁶ This capability allows us to evaluate the impact of electron transfer on both structures and energetics quantitatively. We first examine the structural and energetic changes upon the complexation of benzene with NO^+ and NO_2^+ without any electron transfer between monomers. Results (A1 and B1 in Figure 1) show that if there were no electron transfer, the interaction would be purely electrostatic with no obvious difference between NO^+ and NO_2^+ , which would approach the aromatic ring in parallel. In both cases, the vertical distances are around 3.0 Å, about the sum of the van der Waals radii of 3.25 Å.²² The N–O stretching vibrational frequencies are close to but slightly blue-shifted from those of monomers. Accordingly, the N–O bond distances shorten negligibly, while the C–C bonds in benzene lengthen insignificantly. It should be noted that our vibrational frequency for NO^+ (2400 cm^{-1}) is higher than the previous experimental value 2272 cm^{-1} ,²¹ which was measured in salt. The most recent experimental standard, however, recommends 2344 cm^{-1} for NO^+ in atmosphere which is comparable to our number computed in vacuum. Another support for the reliability of the theoretical level used here comes from the neutral NO in the gaseous phase. At the B3LYP/cc-pVTZ level, the scaled vibrational frequency is 1915 cm^{-1} , compared with the experimental data value of 1875 cm^{-1} .

The regular DFT geometry optimizations with electron transfer considered result in structures A2 and B2 in Figure 1.

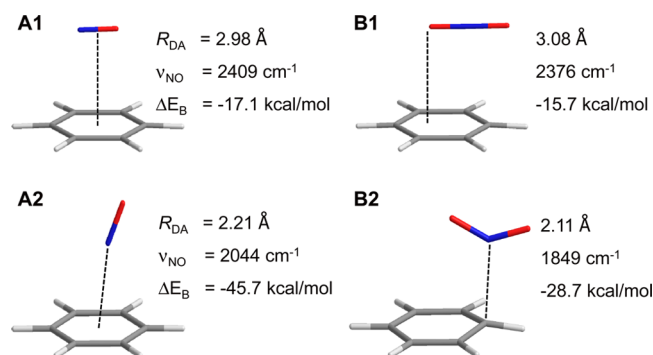


Figure 1. Optimal complexes from the interactions of benzene with NO^+ and NO_2^+ at the B3LYP/cc-pVTZ level. A1 and B1, resulted from the BLW optimizations, correspond to nonbond states where the charge transfer between interacting moieties is quenched. A2 and B2, derived from regular DFT optimizations, refer to real cases with charge transfer considered.

The optimal structure of the $[\text{C}_6\text{H}_6\text{NO}]^+$ complex is very similar to the crystal structure, where the intermolecular separation is about 2.1 Å and well below the sum of the van der Waals radii of 3.25 Å.²² NO^+ is slightly tilted but points to the center of the aromatic ring. In the complex, the N–O bond distance increases by 0.042 Å, while the stretching vibrational frequency significantly red-shifts by 465 cm^{-1} . Differently, NO_2^+ bends and uses the nitrogen atom to approach one carbon atom, instead of the overall π ring. The targeted carbon atom slightly pyramids. With the N–C distance of 2.109 Å, however, $[\text{C}_6\text{H}_6\text{NO}_2]^+$ is still a weakly bound complex.

Experimentally, Friedrich and Person proposed the experimental measure of the degree of charge transfer (Z) from the aromatic donor to the NO^+ acceptor in nitrosonium complexes based on the spectral variations of the N–O stretching frequencies as^{21,67}

$$Z = \frac{\nu_{\text{NO}^+}^2 - \nu_{\text{C}}^2}{\nu_{\text{NO}^+}^2 - \nu_{\text{NO}}^2} \quad (8)$$

where ν_{NO^+} , ν_{C} , and ν_{NO} refer to N–O frequencies for the free NO^+ , the nitrosonium complex, and the neutral NO, respectively. Table 1 compares our population analyses based

Table 1. Amount of Charges (e) Transferred from Benzene to Electrophiles

E	this work		Gwaltney et al. ²⁶	expt. (eq 8) ²¹
	Mulliken	NPA		
NO^+	0.58	0.52	0.69	0.52
NO_2^+	0.71	0.64	0.71	N/A

on the Mulliken scheme and the natural orbital method⁶⁸ with others. Both theoretical analyses and experimental estimates concur that there is considerable (about half electron) electron transfer from benzene to NO^+ . While there is lack of experimental measure for the nitronium complex, computations show that there is 20% more of electrons transferred from benzene to NO_2^+ . This partially explains the dramatically different reactivities of NO^+ and NO_2^+ toward arene. In accord, the antisymmetric stretching vibrational frequency of NO_2^+ red-shifts by 527 cm^{-1} upon the complexation with benzene, and the N–O bond distances stretches by 0.053 Å. Interestingly, the population and frequency analyses are in contrast to the

binding energies (Table 2), as the stabilization energy of the π -bonding in the complex $[\text{C}_6\text{H}_6\text{NO}_2]^+$ is only two-thirds of the

Table 2. Energy Terms to the Formation of π Complexes (kcal/mol)

energy term	$[\text{C}_6\text{H}_6\text{NO}]^+$	$[\text{C}_6\text{H}_6\text{NO}_2]^+$
ΔE_{def}	3.16	35.18
ΔE_{HL}	15.05	29.23
ΔE_{pol}	-13.84	-17.35
ΔE_{CT}	-50.07	-75.76
ΔE_{B}	-45.70	-28.70

analogous $[\text{C}_6\text{H}_6\text{NO}]^+$ complex.²⁶ We note that our computed binding energy for $[\text{C}_6\text{H}_6\text{NO}]^+$ (45.7 kcal/mol) is in good agreement with the experimental estimate of 44 ± 5 kcal/mol.⁶⁹

BLW Energy Decomposition Analyses. To understand the disparity between the reactivity and the binding energy for the benzene complexes with NO^+ and NO_2^+ , we performed energy decomposition analyses⁷⁰ to decipher the physical principles governing the π -cation interactions in $[\text{C}_6\text{H}_6\text{E}]^+$.⁷¹ This is accomplished by decomposing the intermolecular interaction energy in a series of successive but hypothetical steps which are characteristic of the reorganization of electron densities. We first assume that monomers experience certain unfavorable geometry deformations from their respective free and optimal structures to the distorted geometries in the optimal complex structure (ΔE_{def}). Then, we bring the distorted monomers together to form the complex without further perturbing the structures of monomers, but all monomer electron densities are frozen. The energy change in this step, similar to many other schemes, is defined as the Heitler–London energy (ΔE_{HL}) which is essentially composed of electrostatic and Pauli exchange interactions. The next step is to the redistribution (polarization) of electron density within each monomer because of the electric field imposed by the other monomer. This is an energy-lowering step for the complex (ΔE_{pol}). Finally, we extend the electron movement from individual monomers to the whole complex which further stabilizes the complex (ΔE_{CT}). Thus, the binding energy (ΔE_{B}) is decomposed as

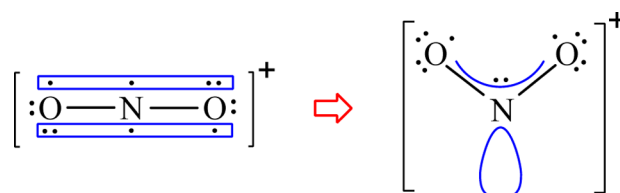
$$\begin{aligned}\Delta E_{\text{B}} &= E(\Psi_{\text{AB}}) - E(\Psi_{\text{A}}) - E(\Psi_{\text{B}}) + \text{BSSE} \\ &= \Delta E_{\text{def}} + \Delta E_{\text{HL}} + \Delta E_{\text{pol}} + \Delta E_{\text{CT}}\end{aligned}\quad (9)$$

where the basis set superposition error (BSSE) is included into the charge transfer energy term. Table 2 compiled the energy terms contributing to the formation of π complexes.

The initial observation reveals surprisingly high charge transfer stabilization energy. Benzene is a nonpolar molecule with a quadrupole moment, and it has been assumed that the electrostatic interaction between the cation and the quadrupole charge distribution of the aromatic is of prime importance in the cation- π interactions.^{72,73} Our previous study of π -cation complexes of benzene with simple cations (Li^+ , Na^+ , K^+ , NH_4^+ , and $\text{N}(\text{CH}_3)_4^+$) based on the same procedure showed that the polarization of benzene contributes about 50% to the interaction energies while the charge transfer plays a minor role.⁴⁵ But in the present cases, the charge transfer stabilization energy is even higher than total binding energy. This strongly implies the significant single electron transfer from benzene to NO^+ and NO_2^+ . Remarkably, the charge transfer effect stabilizes

the $[\text{C}_6\text{H}_6\text{NO}_2]^+$ complex by 75.8 kcal/mol, compared with 50.1 kcal/mol in $[\text{C}_6\text{H}_6\text{NO}]^+$. In accord with the population analyses in Table 1, the difference in charge transfer energies partially explains the disparity of two species in the electrophilic reactions with aromatic rings.

With 50% more charge transfer energy than the nitronium complex, why is the nitronium complex much less stable in the end? Table 2 shows the deformation cost and the Pauli repulsion as the culprits. While the higher Pauli repulsion in $[\text{C}_6\text{H}_6\text{NO}_2]^+$ than in $[\text{C}_6\text{H}_6\text{NO}]^+$ is due to the shorter donor–acceptor distance, the lower overall binding energy in $[\text{C}_6\text{H}_6\text{NO}_2]^+$ is largely due to the unfavorable deformation cost of NO_2^+ (35.2 kcal/mol vs 3.2 kcal/mol for NO^+). A free NO_2^+ takes a linear geometry with two three-center-four-electron Π bonds. In the process of approaching benzene, it gradually bends to a V-type structure with only one three-center-four-electron Π bond and a vacant σ orbital centered on nitrogen as follows



Based on the above scheme, it seems better to regard $[\text{C}_6\text{H}_6\text{NO}_2]^+$ as a pre- σ rather than a π complex. This can be further confirmed by visualizing the electron density change in the process of polarization and electron transfer (Figure 2). For

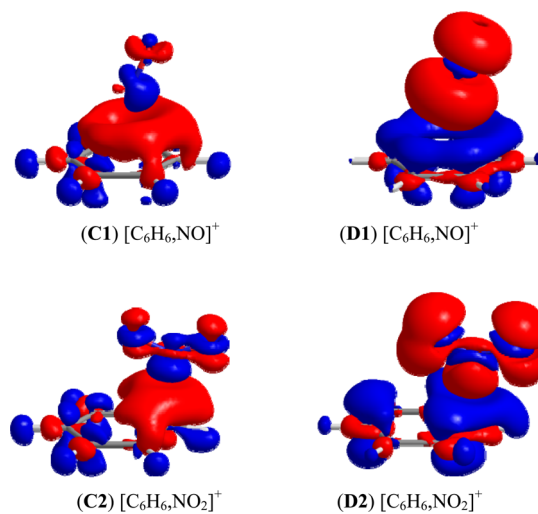


Figure 2. Electron density difference (EDD) maps showing (C) the polarization within monomers and (D) the electron transfer between monomers with the isodensity 0.002 au at the B3LYP/cc-pVTZ level. The red or blue colors denote the gain or loss of electron density.

benzene, the polarization results from the $\sigma \rightarrow \pi^*$ excitation, and the overall effect is the electron density shift from hydrogen (σ orbitals) to carbon (π orbitals). For the electrophiles, polarization moves electron density from nitrogen to oxygen atom(s). Notably, NO^+ uses its nearly degenerate π antibonding orbitals to accommodate the incoming electron density, while NO_2^+ bends and uses its vacant σ (Nsp^2) orbital to accept electron density.

Two-State Model Analyses. The BLW energy decomposition analyses showed that the electron transfer energies in

$[\text{C}_6\text{H}_6\text{E}]^+$ ($\text{E} = \text{NO}, \text{NO}_2$) complexes are much higher than the binding energies and even fall in the range of single bond energies (50–120 kcal/mol). Moreover, the supposedly dominating electrostatic attraction is actually overwhelmed by the Pauli repulsion, leading to an overall destabilizing Heitler–London energy term. Thus, we question whether the π complexes are dominated by the no-bond structure $[\text{C}_6\text{H}_6\text{E}]^+$ (a) like many π -cation complexes or the charge transfer structure $[\text{C}_6\text{H}_6^+-\text{E}]$ (b) with a covalent bond between benzene and electrophiles. We computed their individual energies, and Table 3 listed the major results. Computations

Table 3. Structural Energies (a.u.), Coefficients, And Weights in the Two-State Configuration Interaction (CI) Method with the Coupling Energy (eV)

	E = NO		E = NO ₂	
	$[\text{C}_6\text{H}_6\text{E}]^+$	$[\text{C}_6\text{H}_6^+-\text{E}]$	$[\text{C}_6\text{H}_6\text{E}]^+$	$[\text{C}_6\text{H}_6^+-\text{E}]$
energy	−359.60495	−359.63720	−434.29026	−434.41445
coeff.	0.5414	0.6982	−0.3321	0.8533
weight	40.3%	59.7%	19.1%	80.9%
E_1 (CI)	−359.68584		−434.43662	
H_{DA}	1.32		0.60	

show that for both complexes of $[\text{C}_6\text{H}_6\text{E}]^+$, the charge-transfer state indeed has lower energy and thus larger contribution to the ground state than the no-bond state. The higher structural weight from the aromatic cation-radical (C_6H_6^+) than from the neutral benzene also explains why the optimal $[\text{C}_6\text{H}_6\text{NO}]^+$ structure does not adopt a C_{6v} symmetry. Because of the Jahn–Teller distortion in C_6H_6^+ and large structural weight of state a, $[\text{C}_6\text{H}_6\text{NO}]^+$ exhibits a tilted NO rather than a perpendicular orientation of C_{6v} symmetry, though the energy gap seems trivial (the C_{6v} structure is <1 kcal/mol unstable than the NO tilted minimum structure). Table 3 also revealed the strong coupling interaction between the two diabatic states. We note, however, that in the electron transfer theory, the electronic coupling energy particularly refers to the geometry where two states are of the same energy. Figure 3 plots the bonding orbitals between benzene and electrophiles in the charge-transfer state. For $[\text{C}_6\text{H}_6^+-\text{NO}]$, we plotted one pair of orbitals

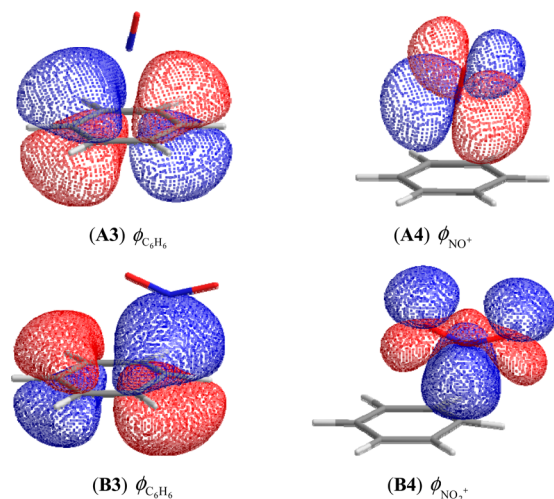


Figure 3. Fragment orbitals involved in the benzene-electrophile bond in the charge transferred state of (A) $[\text{C}_6\text{H}_6^+-\text{NO}]$ and (B) $[\text{C}_6\text{H}_6^+-\text{NO}_2]$ with the isodensity 0.02 au at the B3LYP/cc-pVTZ level.

as there is another pair which is generated by rotating A3 and A4 by 90°. These figures reinforce the conclusion that NO^+ uses its π orbitals to interact with benzene, while NO_2^+ bends to create a vacant σ orbital mainly on the nitrogen atom which interacts with a lobe of a π orbital of benzene.

With the two-state VB-CI energies listed in Table 3, we can derive the binding energies at this theoretical level, which are −40.04 kcal/mol and −30.70 kcal/mol for the complexes $[\text{C}_6\text{H}_6\text{NO}]^+$ and $[\text{C}_6\text{H}_6\text{NO}_2]^+$ without the correction of BSSE. These data are in reasonable agreement with the B3LYP/cc-pVTZ energies listed in Table 2.

To fully explore the two-state model, we need to derive the energy profiles of both diabatic states together with the adiabatic state along the reaction coordinate. Considering that there is little structural change in the complexation of benzene with NO^+ , and the tilted optimal structure is only slightly more stable than the C_{6v} structure, we started from the optimal monomers of benzene and NO^+ , and let the latter vertically approach the center of benzene with the nitrogen end. Figure 4

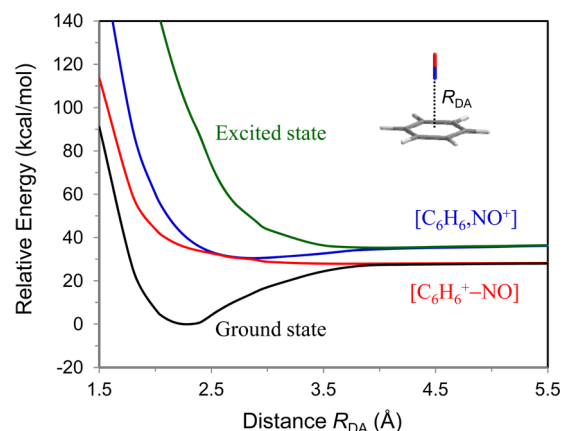


Figure 4. Energy profiles of diabatic and adiabatic states along the donor–acceptor distance for $[\text{C}_6\text{H}_6-\text{NO}]^+$.

shows the computation results, from which significant findings can be garnered. First, the plot is very different from the previous qualitative illustration.²⁶ Second, benzene and NO^+ change their charge states with an electron jumping in their outer spheres (at ~ 2.6 Å). At this point, the electronic coupling energy is 1.06 eV, which is comparable to the experimental estimate 1.4 ± 0.5 eV.²³ Third, at the infinite distance, the charge transfer state is more stable than the no-bond state. This is consistent with the experimental evidence that the ionization energy (IE) of benzene at the gas phase (9.24 eV) is slightly lower than that of NO (9.26 eV) and NO_2 (9.59 eV). Fourthly, because of the lower IE of benzene than NO and the bonding interaction in the short distance, the energy curve of the no-bond diabatic state (blue line) is completely within the energy curve of the charge transfer diabatic state (red line) except the overlapping area at ~ 2.6 Å. Consequently, the electron transfer reaction between benzene and NO^+ falls in the “inverted region” in Marcus theory.^{74,75} The existence of the Marcus inverted region was first experimentally verified by Miller et al. in 1984 in a molecular system where donor and acceptor are kept at a constant distance.^{76,77} Finally, the no-bond state has a shallow minimum at ~ 3.5 Å. Yet, it is the strong coupling between the two states that remarkably stabilizes the complex of $[\text{C}_6\text{H}_6-\text{NO}]^+$. This perfectly fits the definition of charge-shift (CS) bonds by Shaik and co-workers.^{78–80}

CONCLUSION

Electrophiles NO_2^+ and NO^+ have very different reactivity toward aromatic donors, though they have similar inherent physical properties. Compared with previous computational studies, the present work has the significant advantage of being able to derive the strictly electron-localized diabatic states self-consistently. Our analyses suggest the use of different bonding orbitals in the π complexes $[\text{C}_6\text{H}_6\text{NO}]^+$ and $[\text{C}_6\text{H}_6\text{NO}_2]^+$ being the key. NO^+ uses its degenerate anti π orbitals to interact with the two degenerate HOMOs of benzene, and the evolution from the π complex to the σ complex thus concerns the orbital switch, which is energetically unfavorable. In contrast, in the process of approaching benzene, NO_2^+ gradually deforms and breaks one three-center-four-electron π bond to generate a σ vacant orbital centered on the nitrogen atom, and uses it to interact with one lobe of a HOMO of benzene. The consequences are, though NO_2^+ has seemingly lower binding energy than NO^+ to benzene, it has much higher charge transfer stabilization energy thus higher chemical reactivity than NO^+ ; the so-called π complex $[\text{C}_6\text{H}_6\text{NO}_2]^+$ is more like a pre- σ complex, and its change to the σ complex is thus nearly barrierless.

While the electron transfer (ET) process in electrophilic aromatic nitrosation and nitration is often described with one pre-ET (no-bond) $[\text{C}_6\text{H}_6\text{E}^+]$ and one post-ET (charge-transfer) $[\text{C}_6\text{H}_6^+-\text{E}]$ diabatic states within the two state model, our ab initio computations showed that the energy profile of the no-bond state is contained by that of the charge transfer state and both energy profiles meet at an outer sphere distance. This indicates that these outer-sphere ET reactions fall in the Marcus inverted region.⁷⁴ Consequently, the aromatic nitrosation and nitration can be described as follows. Because of the lower IE of benzene than NO^+ and NO_2^+ , reactions start from neutral benzene and E^+ ($\text{E} = \text{NO}, \text{NO}_2$) which have a higher energy than the combination of benzene cation and E . With the approaching of the electrophiles to benzene, there is an electron transfer at the outer sphere, and the system now is dominated by the charge-transfer state $[\text{C}_6\text{H}_6^+-\text{E}]$. The strong coupling between the two diabatic states in the π complexes is responsible for the stabilization of the complexes.

AUTHOR INFORMATION

Corresponding Author

*E-mail: yirong.mo@wmich.edu.

Notes

The authors declare no competing financial interest.

ACKNOWLEDGMENTS

This work was supported by the U.S. National Science Foundation under the Grants CHE-1055310 and CNS-1126438.

REFERENCES

- (1) Taylor, R. *Electrophilic Aromatic Substitution*; John Wiley: New York, 1990.
- (2) Olah, G. A.; Schlossberg, R. H.; Porter, R. D.; Mo, Y. K.; Kelly, D. P.; Mateescu, G. Stable Carbocations. CXXIV. Benzenium Ion and Monoalkylbenzenium Ions. *J. Am. Chem. Soc.* **1972**, *94*, 2034–2043.
- (3) Corey, E. J.; Barcza, S.; Klotmann, G. Directed Conversion of the Phenoxy Grouping into a Variety of Cyclic Polyfunctional Systems. *J. Am. Chem. Soc.* **1969**, *91*, 4782–4786.
- (4) Kenner, J. Oxidation and Reduction in Chemistry. *Nature* **1945**, *156*, 369–370.
- (5) Weiss, J. Simple Electron Transfer Processes in Systems of Conjugated Double Bonds. *Trans. Faraday Soc.* **1946**, *42*, 116–121.
- (6) Hughes, E. D.; Ingold, C. K.; Reed, R. I. Kinetics of Aromatic Nitration: The Nitronium Ion. *Nature* **1946**, *158*, 448–449.
- (7) Olah, G. A.; Malhotra, R.; Narang, S. C. *Nitration: Methods and Mechanisms*; VCH Publishers: New York, 1989.
- (8) Schofield, K. *Aromatic Nitration*; Cambridge University Press: Cambridge, U.K., 1980.
- (9) Williams, D. L. H. *Nitrosation*; Cambridge University Press: Cambridge, U.K., 1988.
- (10) Bosch, E.; Kochi, J. K. Direct Nitrosation of Aromatic Hydrocarbons and Ethers with the Electrophilic Nitrosonium Cation. *J. Org. Chem.* **1994**, *59*, 5573–5586.
- (11) Chiavarino, B.; Crestoni, M. E.; Fornarini, S.; Lemaire, J.; Maitre, P.; MacAleese, L. π -Complex Structure of Gaseous Benzene–NO Cations Assayed by IR Multiple Photon Dissociation Spectroscopy. *J. Am. Chem. Soc.* **2006**, *128*, 12553–12561.
- (12) Balzani, V. *Electron Transfer in Chemistry*; Wiley-VCH: Weinheim, Germany, 2001.
- (13) Politzer, P.; Jayasurya, K.; Sjöberg, P.; Laurence, P. R. Properties of Some Possible Intermediate Stages in the Nitration of Benzene and Toluene. *J. Am. Chem. Soc.* **1985**, *107*, 1174–1177.
- (14) Szabó, K. J.; Hörnfeldt, A.-B.; Gronowitz, S. Theoretical Study on Mechanism and Selectivity of Electrophilic Aromatic Nitration. *J. Am. Chem. Soc.* **1992**, *114*, 6827–6834.
- (15) Liljenberg, M.; Brinck, T.; Herschend, B.; Rein, T.; Rockwell, G.; Svensson, M. Validation of a Computational Model for Predicting the Site for Electrophilic Substitution in Aromatic Systems. *J. Org. Chem.* **2010**, *75*, 4696–4705.
- (16) de Queiroz, J. F.; Carneiro, J. W. D.; Sabino, A. A.; Sparrapan, R.; Eberlin, M. N.; Esteves, P. M. Electrophilic Aromatic Nitration: Understanding Its Mechanism and Substituent Effects. *J. Org. Chem.* **2006**, *71*, 6192–6203.
- (17) Esteves, P. M.; Carneiro, J. W. d. M.; Cardoso, S. P.; Barbosa, A. G. H.; Laali, K. K.; Rasul, G.; Prakash, G. K. S.; Olah, G. A. Unified Mechanistic Concept of Electrophilic Aromatic Nitration: Convergence of Computational Results and Experimental Data. *J. Am. Chem. Soc.* **2003**, *125*, 4836–4849.
- (18) Ebersson, L. *Electron Transfer Reactions in Organic Chemistry*; Springer-Verlag: Berlin, Germany, 1987.
- (19) Ebersson, L.; Radner, F. Electron-Transfer Mechanisms in Electrophilic Aromatic Nitration. *Acc. Chem. Res.* **1987**, *20*, 53–59.
- (20) Ebersson, L.; Radner, F. Electron Transfer Reactions in Organic Chemistry. VI. Possible Role of Electron Transfer in Aromatic Nitration by Nitrosonium and Nitronium Ion. *Acta Chem. Scand.* **1984**, *B38*, 861–870.
- (21) Kim, E. K.; Kochi, J. K. Charge-Transfer Structures of Aromatic Electron Donor-Acceptor Complexes Leading to Electron Transfer with the Electrophilic Nitrosonium Cation. *J. Am. Chem. Soc.* **1991**, *113*, 4962–4974.
- (22) Rosokha, S. V.; Kochi, J. K. Mechanism of Inner-Sphere Electron Transfer via Charge-Transfer (Precursor) Complexes. Redox Energetics of Aromatic Donors with the Nitrosonium Acceptor. *J. Am. Chem. Soc.* **2001**, *123*, 8985–8999.
- (23) Rosokha, S. V.; Kochi, J. K. Strong Electronic Coupling in Intermolecular (Charge-Transfer) Complexes. Mechanistic Relevance to Thermal and Optical Electron Transfer from Aromatic Donors. *New J. Chem.* **2002**, *26*, 851–860.
- (24) Rosokha, S. V.; Kochi, J. K. Fresh Look at Electron-Transfer Mechanisms via the Donor/Acceptor Bindings in the Critical Encounter Complex. *Acc. Chem. Res.* **2008**, *41*, 641–653.
- (25) March, J. *Advanced Organic Chemistry*; McGraw-Hill: New York, 1984.
- (26) Gwaltney, S. R.; Rosokha, S. V.; Head-Gordon, M.; Kochi, J. K. Charge-Transfer Mechanism for Electrophilic Aromatic Nitration and Nitrosation via the Convergence of (ab Initio) Molecular-Orbital and Marcus-Hush Theories with Experiments. *J. Am. Chem. Soc.* **2003**, *125*, 3273–3283.

- (27) Challis, B. C.; Higgins, R. J.; Lawson, A. J. Chemistry of Nitroso Compounds. III. Nitrosation of Substituted Benzenes in Concentrated Acids. *J. Chem. Soc., Perkin Trans. 2* **1972**, 1831–6.
- (28) Marcus, R. A. Electron-Transfer Reactions in Chemistry: Theory and Experiment (Nobel Lecture). *Angew. Chem., Int. Ed.* **1993**, 32, 1111–1121.
- (29) Mulliken, R. S. Molecular Compounds and Their Spectra. II. *J. Am. Chem. Soc.* **1952**, 74, 811–824.
- (30) Hush, N. S. Adiabatic Theory of Outer-Sphere Electron-Transfer Reactions in Solutions. *Trans. Faraday Soc.* **1961**, 57, 557–580.
- (31) Marcus, R. A. Chemical and Electrochemical Electron-Transfer Theory. *Annu. Rev. Phys. Chem.* **1964**, 15, 155–196.
- (32) Newton, M. D. Electron Transfer: Theoretical Models and Computational Implementation. In *Electron Transfer in Chemistry*; Balzani, V., Ed.; Wiley-VCH Verlag GmbH: Weinheim, Germany, 2001; Vol. 1, pp 3–63.
- (33) Brunschwig, B. S.; Sutin, N. Energy Surfaces, Reorganization Energies, and Coupling Elements in Electron Transfer. *Coord. Chem. Rev.* **1999**, 187, 233–254.
- (34) Newton, M. D. Quantum Chemical Probes of Electron-Transfer Kinetics: The Nature of Donor-Acceptor Interactions. *Chem. Rev.* **1991**, 91, 767–792.
- (35) Migliore, A.; Corni, S.; Di Felice, R.; Molinari, E. First-Principles DFT Calculations of Electron Transfer Rates in Azurin Dimers. *J. Chem. Phys.* **2006**, 124, 064501.
- (36) Lee, S.-J.; Chen, H.-C.; You, Z.-Q.; Liu, K.-L.; Chow, T. J.; Hsu, C.-P. Theoretical Characterization of Photoinduced Electron Transfer in Rigidly Linked Donor-Acceptor Molecules: The Fragment Charge Difference and the Generalized Mulliken–Hush Schemes. *Mol. Phys.* **2010**, 108, 2775–2789.
- (37) Dederichs, P. H.; Bluegel, S.; Zeller, R.; Akai, H. Ground States of Constrained Systems: Application to Cerium Impurities. *Phys. Rev. Lett.* **1984**, 53, 2512–2515.
- (38) Wu, Q.; Van Voorhis, T. Extracting Electron Transfer Coupling Elements from Constrained Density Functional Theory. *J. Chem. Phys.* **2006**, 125, 164105.
- (39) Shaik, S.; Shurki, A. Valence Bond Diagrams and Chemical Reactivity. *Angew. Chem., Int. Ed.* **1999**, 38, 586–625.
- (40) Cooper, D. L. *Valence Bond Theory*; Elsevier: Amsterdam, The Netherlands, 2002.
- (41) Gallup, G. A.; Vance, R. L.; Collins, J. R.; Norbeck, J. M. Practical Valence-Bond Calculations. *Adv. Quantum Chem.* **1982**, 16, 229–272.
- (42) Shaik, S. S.; Hiberty, P. C. *A Chemist's Guide to Valence Bond Theory*; Wiley: Hoboken, NJ, 2008.
- (43) Wu, W.; Su, P.; Shaik, S.; Hiberty, P. C. Classical Valence Bond Approach by Modern Methods. *Chem. Rev.* **2011**, 111, 7557–93.
- (44) Mo, Y.; Peyerimhoff, S. D. Theoretical Analysis of Electronic Delocalization. *J. Chem. Phys.* **1998**, 109, 1687–1697.
- (45) Mo, Y.; Song, L.; Lin, Y. The Block-Localized Wavefunction (BLW) Method at the Density Functional Theory (DFT) Level. *J. Phys. Chem. A* **2007**, 111, 8291–8301.
- (46) Mo, Y. Computational Evidence that Hyperconjugative Interactions Are Not Responsible for the Anomeric Effect. *Nat. Chem.* **2010**, 2, 666–671.
- (47) Cembran, A.; Payaka, A.; Lin, Y.-L.; Xie, W.; Mo, Y.; Song, L.; Gao, J. A Non-Orthogonal Block-Localized Effective Hamiltonian Approach for Chemical and Enzymatic Reactions. *J. Chem. Theory Comput.* **2010**, 6, 2242–2251.
- (48) Cembran, A.; Song, L.; Y., M.; Gao, J. Block-Localized Density Functional Theory (BL-DFT), Diabatic Coupling, and Its Use in Valence Bond Theory for Representing Reactive Potential Energy Surfaces. *J. Chem. Theory Comput.* **2009**, 5, 2702–2716.
- (49) Mo, Y.; Gao, J. Ab Initio QM/MM Simulations with a Molecular Orbital-Valence Bond (MOVb) Method: Application to An S_N2 Reaction in Water. *J. Comput. Chem.* **2000**, 21, 1458–1469.
- (50) Mo, Y.; Gao, J. An Ab Initio Molecular Orbital-Valence Bond (MOVb) Method for Simulating Chemical Reactions in Solution. *J. Phys. Chem.* **2000**, 104, 3012–3020.
- (51) Mo, Y.; Song, L.; Liu, M.; Lin, Y.; Cao, Z.; Wu, W. Block-Localized Wavefunction (BLW) Based Two-State Approach for Charge Transfers between Phenyl Rings. *J. Chem. Theory Comput.* **2012**, 8, 800–805.
- (52) Song, L.; Mo, Y.; Gao, J. An Effective Hamiltonian Molecular Orbital-Valence Bond (MOVb) Approach for Chemical reactions Applied to the Nucleophilic Substitution Reaction of Hydrosulfide Ion and Chloromethane. *J. Chem. Theory Comput.* **2009**, 5, 174–185.
- (53) Stoll, H.; Preuss, H. On the Direct Calculation of Localized HF Orbitals in Molecular Clusters, Layers and Solids. *Theor. Chim. Acta* **1977**, 46, 11–21.
- (54) Stoll, H.; Wagenblast, G.; Preuss, H. On the Use of Local Basis Sets for Localized Molecular Orbitals. *Theor. Chim. Acta* **1980**, 57, 169–178.
- (55) Mehler, E. L. Self-Consistent, Nonorthogonal Group Function Approximation for Polyatomic Systems. I. Closed Shells. *J. Chem. Phys.* **1977**, 67, 2728–2739.
- (56) Mehler, E. L. Self-Consistent, Nonorthogonal Group Function Approximation for Polyatomic Systems. II. Analysis of Noncovalent Interactions. *J. Chem. Phys.* **1981**, 74, 6298–6306.
- (57) Gianinetti, E.; Raimondi, M.; Tornaghi, E. Modification of the Roothaan Equations to Exclude BSSE from Molecular Interaction Calculations. *Int. J. Quantum Chem.* **1996**, 60, 157–166.
- (58) Gianinetti, E.; Vandoni, I.; Famulari, A.; Raimondi, M. Extension of the SCF-MI Method to the Case of K Fragments One of Which Is an Open-Shell System. *Adv. Quantum Chem.* **1998**, 31, 251–266.
- (59) Famulari, A.; Gianinetti, E.; Raimondi, M.; Sironi, M. Implementation of Gradient-Optimization Algorithms and Force Constant Computations in BSSE-Free Direct and Conventional SCF Approaches. *Int. J. Quantum Chem.* **1998**, 69, 151–158.
- (60) Khaliullin, R. Z.; Cobar, E. A.; Lochan, R. C.; Bell, A. T.; Head-Gordon, M. Unravelling the Origin of Intermolecular Interactions Using Absolutely Localized Molecular Orbitals. *J. Phys. Chem. A* **2007**, 111, 8753–65.
- (61) Khaliullin, R. Z.; Bell, A. T.; Head-Gordon, M. An Efficient Self-Consistent Field Method for Large Systems of Weakly Interacting Components. *J. Chem. Phys.* **2006**, 124, 204105.
- (62) Mo, Y.; Wu, W.; Zhang, Q. Study of Intramolecular Electron Transfer with a Two-State Model Based on the Orbital Deletion Procedure. *J. Chem. Phys.* **2003**, 119, 6448–6456.
- (63) Schmidt, M. W.; Baldridge, K. K.; Boatz, J. A.; Elbert, S. T.; Gordon, M. S.; Jensen, J. J.; Koseki, S.; Matsunaga, N.; Nguyen, K. A.; Su, S.; Windus, T. L.; Dupuis, M.; Montgomery, J. A. General Atomic and Molecular Electronic Structure System. *J. Comput. Chem.* **1993**, 14, 1347–1363.
- (64) Merrick, J. P.; Moran, D.; Radom, L. An Evaluation of Harmonic Vibrational Frequency Scale Factors. *J. Phys. Chem. A* **2007**, 111, 11683–11700.
- (65) Song, L.; Chen, Z.; Ying, F.; Song, J.; Chen, X.; Su, P.; Mo, Y.; Zhang, Q.; Wu, W. *XMVB 2.0: An Ab Initio Non-Orthogonal Valence Bond Program*; Xiamen University: Xiamen, China, 2012.
- (66) Mo, Y. Geometrical Optimization for Strictly Localized Structures. *J. Chem. Phys.* **2003**, 119, 1300–1306.
- (67) Friedrich, H. B.; Person, W. B. Infrared Spectra of Charge-Transfer Complexes. VI. Theory. *J. Chem. Phys.* **1966**, 44, 2161–2170.
- (68) Reed, A. E.; Weinstock, R. B.; Weinhold, F. Natural Population Analysis. *J. Chem. Phys.* **1985**, 83, 735–746.
- (69) Reents, W. D., Jr.; Freiser, B. S. Gas-Phase Binding Energies and Spectroscopic Properties of Nitrosyl(1+) Charge-Transfer Complexes. *J. Am. Chem. Soc.* **1981**, 103, 2791–2797.
- (70) Mo, Y.; Bao, P.; Gao, J. Intermolecular Interaction Energy Decomposition Based on Block-Localized Wavefunction and Block-Localized Density Functional Theory. *Phys. Chem. Chem. Phys.* **2011**, 13, 6760–6775.

- (71) Hopffgarten, M.; Frenking, G. Energy Decomposition Analysis. *WIREs Comput. Mol. Sci.* **2012**, *2*, 43–62.
- (72) Dougherty, D. A. Cation- π Interactions in Chemistry and Biology: A New View of Benzene, Phe, Tyr, and Trp. *Science* **1996**, *271*, 163–168.
- (73) Mecozzi, S.; West, A. P.; Dougherty, D. A. Cation- π Interactions in Simple Aromatics: Electrostatics Provide a Predictive Tool. *J. Am. Chem. Soc.* **1996**, *118*, 2307–2308.
- (74) Marcus, R. A. On the Theory of Oxidation-Reduction Reactions Involving Electron Transfer. I. *J. Chem. Phys.* **1956**, *24*, 966–978.
- (75) Grampp, G. The Marcus Inverted Region From Theory to Experiment. *Angew. Chem., Int. Ed.* **1993**, *32*, 691–693.
- (76) Miller, J. R.; Calcaterra, L. T.; Closs, G. L. Intramolecular Long-Distance Electron Transfer in Radical Anions. The Effects of Free Energy and Solvent on the Reaction Rates. *J. Am. Chem. Soc.* **1984**, *106*, 1983–1985.
- (77) Suppan, P. The Marcus Inverted Region. *Top. Curr. Chem.* **1992**, *163*, 95–130.
- (78) Shaik, S.; Maitre, P.; Sini, G.; Hiberty, P. C. The Charge-Shift Bonding Concept. Electron-Pair Bonds with Very Large Ionic-Covalent Resonance Energies. *J. Am. Chem. Soc.* **1992**, *114*, 7861–7866.
- (79) Wu, W.; Gu, J.; Song, J.; Shaik, S.; Hiberty, P. C. The ‘Inverted’ Bond in [1.1.1] Propellane Is a Charge-Shift Bond. *Angew. Chem., Int. Ed.* **2009**, *48*, 1407–1410.
- (80) Shaik, S.; Danovich, D.; Wu, W.; Hiberty, P. C. Charge-Shift Bonding and Its Manifestations in Chemistry. *Nat. Chem.* **2009**, *1*, 443–449.